PROCEEDINGS OF SCIENCE

Prompt and non-prompt J/ψ production at midrapidity in Pb–Pb collisions at $\sqrt{s_{\rm NN}}$= 5.02 TeV with ALICE

Himanshu Sharma for the ALICE Collaboration [a]

[a] *Institute of Nuclear Physics, Polish Academy of Sciences, Krakow (IFJPAN), Krakow, Poland*

E-mail: himanshu.sharma@cern.ch

J/ψ production is sensitive to the deconfined strongly interacting medium produced in ultrarelativistic nuclear collisions. Measurement of prompt and non-prompt J/ψ, the latter originating from beauty hadron decays, are essential to investigate the parton energy loss in the hot medium and its quark mass dependence. In addition, the production of prompt J/ψ provides a direct comparison with models that include regeneration, which is the dominant production mechanism at low transverse momentum ($p_{\rm T}$) in central collisions at the LHC. In this contribution, recent ALICE results on prompt and non-prompt J/ψ nuclear modification factors ($R_{\rm AA}$), as a function of $p_{\rm T}$ and in several centrality ranges, are discussed. Presented results, obtained by using the full available statistics from Pb–Pb collisions collected at $\sqrt{s_{\rm NN}}$ = 5.02 TeV during the LHC Run 2, are compared with similar measurements from CMS and ATLAS experiments and to theoretical predictions.

Large Hadron Collider Physics Conference (LHCP 2022), 16-20 May 2022

PoS(LHCP2022)339

Charm and anticharm quark pairs ($c\bar{c}$) are produced in the hard scatterings between partons in the initial stages of ultrarelativistic nuclear collisions. Due to their early production, c and $\bar{c}$ quarks experience the complete evolution of the system and bring information on the deconfined phase of strongly interacting matter, known as quark–gluon plasma (QGP). These pairs can hadronize into charmonium states, such as the J/ψ meson, on timescales comparable with the QGP formation time and life span. It is foreseen that the c and $\bar{c}$ quarks experience the Debye color screening [1] or dissociation [2] in the presence of a hot medium, leading to the melting of the charmonium state into its constituents. These effects result in a modification of the J/ψ yield in A–A collisions with respect to the yield in pp collisions at the same collision energy and scaled by the number of binary nucleon–nucleon collisions. A suppression has been measured for J/ψ and heavier charmonium states in heavy-ion collisions with respect to pp at the SPS [3], RHIC [4, 5] and LHC [6–8]. At LHC energies, the density of charm quarks is larger than at RHIC energies by about one order of magnitude [9]. Therefore, uncorrelated c and $\bar{c}$ quarks can combine to form a charmonium state, either in the QGP [10] or at the phase boundary [11]. This production mechanism is known as regeneration. In nuclear collisions at LHC energies, charmonium production in the hot medium is mainly governed by these two mechanisms, namely melting of the early produced charmonia and regeneration at later stages.

J/ψ mesons directly produced in hard parton scatterings and those originating from the decays of heavier charmonium states, such as $\psi(2S)$ and χ_c, are known as prompt J/ψ. In addition, there is a significant contribution to the inclusive J/ψ yield coming from the decays of beauty hadrons, known as non-prompt J/ψ component. Such contribution is $\sim 10\%$ at low transverse momentum (p_{T}) and nearly 50% around $p_{\mathrm{T}} = 20$ GeV/c. In Pb–Pb collisions, prompt and non-prompt J/ψ measurements allow one to quantify the medium effects on c and b quarks, respectively. The prompt J/ψ production provides a direct comparison with models that include regeneration, which is the dominant production mechanism at low p_{T} at the LHC, in central Pb–Pb events. Non-prompt J/ψ measurements represent a useful tool to study beauty quark energy loss in medium. Nuclear modification effects can be quantified by the nuclear modification factor (R_{AA}), which is defined as:

$$R_{\mathrm{AA}}(y, p_{\mathrm{T}}) = \frac{1}{\langle T_{\mathrm{AA}} \rangle} \frac{\mathrm{d}^2 N_{\mathrm{AA}}/\mathrm{d}y\mathrm{d}p_{\mathrm{T}}}{\mathrm{d}^2 \sigma_{\mathrm{pp}}/\mathrm{d}y\mathrm{d}p_{\mathrm{T}}}, \tag{1}$$

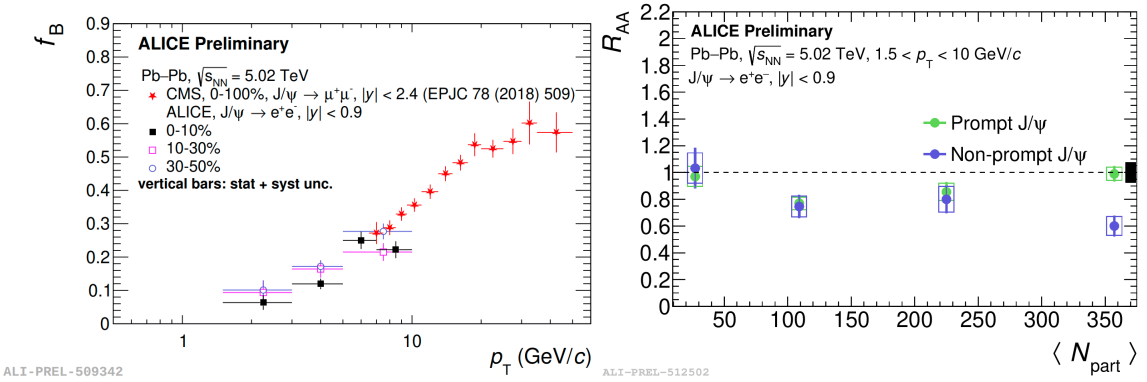

Figure 1: Left: Non-prompt J/ψ fraction (f_{B}) measured in Pb–Pb collisions as a function of p_{T} in several centrality intervals and compared with similar results from the CMS Collaboration [12] in the 0-100% centrality range. Right: R_{AA} of prompt and non-prompt J/ψ as function of $\langle N_{\mathrm{part}} \rangle$ in Pb–Pb collisions at $\sqrt{s_{\mathrm{NN}}}$= 5.02 TeV.

where $\mathrm{d}^2\sigma_{\mathrm{pp}}/\mathrm{d}y\mathrm{d}p_{\mathrm{T}}$ is the J/ψ p_{T} and y double-differential cross section in pp, $\mathrm{d}^2N_{\mathrm{AA}}/\mathrm{d}y\mathrm{d}p_{\mathrm{T}}$ is the J/ψ double-differential yield in Pb–Pb and $\langle T_{\mathrm{AA}}\rangle$ is the average nuclear overlap function, proportional to the number of binary nucleon–nucleon collisions and determined by MC Glauber model simulations [13].

The ALICE detector [14] is able to reconstruct inclusive charmonia at midrapidity and forward rapidity, down to zero p_{T}, through the dielectron and the dimuon decay channels, respectively. At midrapidity ($|y| < 0.9$), track reconstruction is performed by the central barrel detectors, in particular the Time Projection Chamber (TPC) and the Inner Tracking System (ITS) which consist of silicon pixel detectors. Particle identification is based on the measurement of the specific energy loss in the active volume of the TPC, while the innermost layers of the ITS allow a precise determination of the primary and secondary vertex positions. Prompt and non-prompt J/ψ separation is possible down to p_{T} = 1.5 GeV/c at midrapidity in Pb–Pb collisions.

The measurement of the non-prompt J/ψ fraction (f_{B}) is performed by unbinned likelihood fits to the invariant mass (m) and pseudoproper decay length (x) of reconstructed dielectron pairs, as a function of p_{T} ($1.5 < p_{\mathrm{T}} < 10$ GeV/c) in the 0–10%, 10–30% and 30–50% centrality ranges, in Pb–Pb collisions at $\sqrt{s_{\mathrm{NN}}}$= 5.02 TeV. Results are shown in the left panel of Fig. 1. The non-prompt J/ψ fraction increases with p_{T} showing no clear centrality dependence. Measurements are consistent with CMS results [12] in the overlapping p_{T} range.

The nuclear modification factor of prompt and non-prompt J/ψ in $1.5 < p_{\mathrm{T}} < 10$ GeV/c has been measured in different centrality intervals and it is displayed in the right panel of Fig. 1 as a function of the average number of participant nucleons, $\langle N_{\mathrm{part}}\rangle$. Similar R_{AA} values for prompt and non-prompt J/ψ have been observed from peripheral (50–90%) to semicentral (10–30%) collisions. A strong suppression has been observed for non-prompt J/ψ in most central collisions (0–10%), while the prompt J/ψ R_{AA} is compatible with unity.

Figure 2 shows the R_{AA} of prompt (left) and non-prompt (right) J/ψ measured as a function of p_{T} in the 0–10%, 10–30% and 30–50% centrality ranges. J/ψ production is significantly suppressed for p_{T} larger than 5 GeV/c in all centrality ranges for both prompt and non-prompt J/ψ. For p_{T} smaller than 5 GeV/c, the R_{AA} increases to unity moving towards central collisions for prompt J/ψ, and in the 0–10% centrality class the non-prompt J/ψ yield is more suppressed than the prompt one.

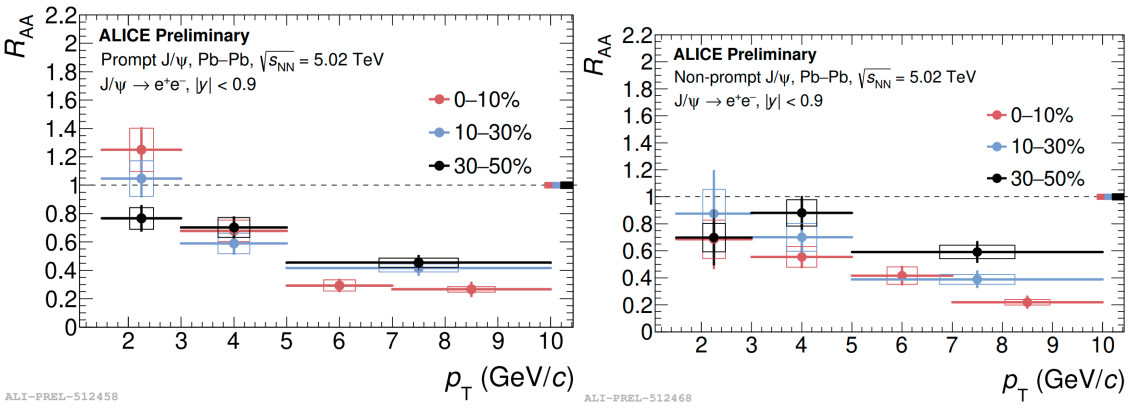

Figure 2: Prompt (left) and non-prompt (right) J/ψ R_{AA} as a function of p_{T} for different centrality intervals in Pb–Pb collisions at $\sqrt{s_{\mathrm{NN}}}$= 5.02 TeV.

Prompt and non-prompt J/ψ R_{AA}, in the 0–10% most central events, are compared with similar measurements performed by the CMS [12] and ATLAS [15] Collaborations, as well as to

theoretical model predictions, as shown in Fig. 3. Prompt and non-prompt J/ψ $R_{\rm AA}$ are consistent with CMS and ATLAS results at high $p_{\rm T}$. Theoretical models, including several nuclear matter effects, describe the $R_{\rm AA}$ of prompt and non-prompt J/ψ in the most central collisions, as shown in Fig 3. The statistical hadronization model for charm quarks (SHMc), in which the J/ψ yield is determined at the phase boundary according to thermal weights, reproduces the $R_{\rm AA}$ of prompt J/ψ for $p_{\rm T}$ smaller than 5 GeV/c [16]. However, the predictions largely underestimate the prompt J/ψ $R_{\rm AA}$ above 5 GeV/c. Models including J/ψ dissociation and charm quark energy loss in the QGP are consistent with the prompt J/ψ $R_{\rm AA}$ for $p_{\rm T}$ larger than 5 GeV/c [17, 18]. The non-prompt J/ψ $R_{\rm AA}$ is consistent with non-prompt $\rm D^0$ measurements by ALICE [19] in the 0–10% centrality class. In addition, models including radiative and collisional energy loss mechanisms for beauty quarks describe the measured non-prompt J/ψ $R_{\rm AA}$ within uncertainties [20–22].

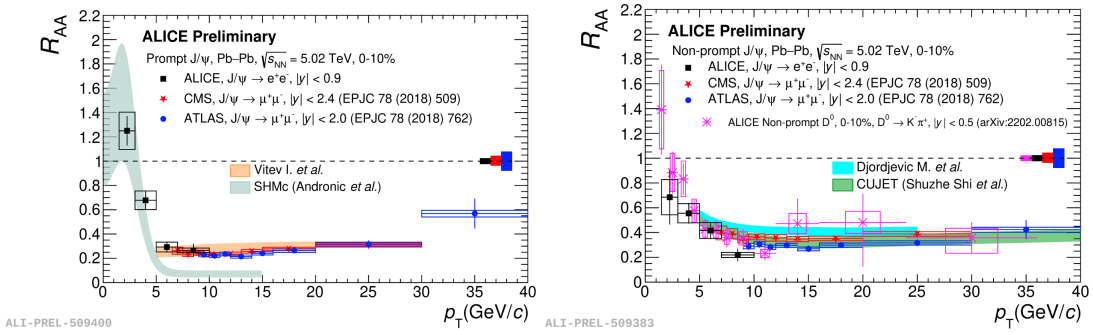

Figure 3: $R_{\rm AA}$ of prompt (left) and non-prompt (right) J/ψ as a function of $p_{\rm T}$ in the 10% most central Pb–Pb collisions at $\sqrt{s_{\rm NN}}$= 5.02 TeV. Data are compared to models [16–18, 21, 22] including several nuclear modification effects. Similar measurements carried out by the CMS [12] and ATLAS [15] Collaborations are also shown along with non-prompt $\rm D^0$ measurements from the ALICE Collaboration [19] at $\sqrt{s_{\rm NN}}$= 5.02 TeV.

In summary, nuclear modification factors of prompt and non-prompt J/ψ are measured at midrapidity in Pb–Pb collisions at $\sqrt{s_{\rm NN}}$= 5.02 TeV. The prompt J/ψ $R_{\rm AA}$ is consistent with model predictions that include regeneration at low $p_{\rm T}$ and dissociation at high $p_{\rm T}$ in the 10% most central events. The non-prompt J/ψ $R_{\rm AA}$ in the 0–10% centrality class is consistent with models including beauty quark energy loss at high $p_{\rm T}$. The results suggest that J/ψ recombination significantly contributes to prompt J/ψ production at low $p_{\rm T}$, in particular in most central collisions. Non-prompt J/ψ measurements are consistent with similar results from non-prompt $\rm D^0$ in most central collisions.

During the LHC Run 3 program (2022–25) [23], Pb–Pb collisions will be collected with an interaction rate of 50 kHz (5 × Run 2) for a target integrated luminosity of 10 $\rm nb^{-1}$ (10 × Run 2). During the second long shut down, ALICE has undergone a major upgrade of the central barrel detectors, improving significantly vertex and track reconstruction precision. In particular, the impact parameter resolution is improved by a factor of three and six in the transverse and beam directions, respectively, and this is crucial for prompt and non-prompt J/ψ measurements. Therefore, more precise measurements for prompt and non-prompt J/ψ are expected at midrapidity in Pb–Pb collisions. Additionally, the newly installed Muon Forward Tracker will allow one to separate prompt and non-prompt J/ψ components at forward rapidity ($-3.6 < \eta < -2.5$) [24].

References

[1] T Matsui and H Satz. In: *Phys. Lett. B* 178 (1986), pp. 416–422.

[2] A Rothkopf. In: *Phys. Rept.* 858 (2020), pp. 1–117. arXiv: 1912.02253 [hep-ph].

[3] NA50 Collaboration. In: *Eur. Phys. J. C* 39 (2005), pp. 335–345. arXiv: hep-ex/0412036.

[4] PHENIX Collaboration. In: *Phys. Rev. C* 84 (2011), p. 054912. arXiv: 1103.6269 [nucl-ex].

[5] STAR Collaboration. In: *Phys. Rev. C* 80 (2009), p. 041902. arXiv: 0904.0439 [nucl-ex].

[6] ALICE Collaboration. In: *Phys. Rev. Lett.* 109 (2012), p. 072301. arXiv: 1202.1383 [hep-ex].

[7] CMS Collaboration. In: *JHEP* 05 (2012), p. 063.

[8] ALICE Collaboration. In: *JHEP* 02 (2020), p. 041. arXiv: 1909.03158 [nucl-ex].

[9] R V Gavai et al. In: *Int. J. Mod. Phys. A* 10 (1995), pp. 2999–3042. arXiv: hep-ph/9411438.

[10] R L Thews et al. In: *Phys. Rev. C* 63 (2001), p. 054905. arXiv: hep-ph/0007323.

[11] P. Braun-Munzinger and J. Stachel. In: *Phys. Lett. B* 490 (2000), pp. 196–202. arXiv: nucl-th/0007059.

[12] CMS Collaboration. In: *Eur. Phys. J. C* 78.6 (2018), p. 509. arXiv: 1712.08959 [nucl-ex].

[13] ALICE Collaboration. In: (2018). URL: https://cds.cern.ch/record/2636623.

[14] ALICE Collaboration. In: *JINST* 3 (2008), S08002.

[15] ATLAS Collaboration. In: *Eur. Phys. J. C* 78.9 (2018), p. 762. arXiv: 1805.04077 [nucl-ex].

[16] A Andronic et al. In: *JHEP* 07 (2021), p. 035. arXiv: 2104.12754 [hep-ph].

[17] Y Makris and I Vitev. In: *JHEP* 10 (2019), p. 111. arXiv: 1906.04186 [hep-ph].

[18] S Aronson et al. In: *Phys. Lett. B* 778 (2018), pp. 384–391. arXiv: 1709.02372 [hep-ph].

[19] ALICE Collaboration. In: (Feb. 2022). arXiv: 2202.00815 [nucl-ex].

[20] S Shi et al. In: *Chinese Physics C* 42.10 (Sept. 2018), p. 104104.

[21] S Shi et al. In: *Chinese Physics C* 43.4 (Apr. 2019), p. 044101.

[22] D Zigic et al. In: (Oct. 2021). arXiv: 2110.01544 [nucl-th].

[23] Z. Citron et al. In: *CERN Yellow Rep. Monogr.* 7 (2019), pp. 1159–1410. arXiv: 1812.06772 [hep-ph].

[24] ALICE Collaboration. Tech. rep. Geneva: CERN, 2013. URL: https://cds.cern.ch/record/1592659.

PoS(LHCP2022)339